

The Decay $\bar{B} \rightarrow \bar{K}\ell^+\ell^-$ at Low Hadronic Recoil and Model-Independent $\Delta B = 1$ Constraints

Christoph Bobeth

*Institute for Advanced Study & Excellence Cluster Universe,
Technische Universität München, D-85748 Garching, Germany*

Gudrun Hiller, Danny van Dyk, and Christian Wacker

Institut für Physik, Technische Universität Dortmund, D-44221 Dortmund, Germany

Abstract

We study the decay $\bar{B} \rightarrow \bar{K}\ell^+\ell^-$ for $\ell = e, \mu, \tau$ with a softly recoiling kaon, that is, for high dilepton invariant masses $\sqrt{q^2}$ of the order of the b -quark mass. This kinematic region can be treated within an operator product expansion and simplified using heavy quark symmetry, leading to systematic predictions for heavy-to-light processes such as $\bar{B} \rightarrow \bar{K}^{(*)}\ell^+\ell^-$. We show that the decay rates of both $\bar{B} \rightarrow \bar{K}^*\ell^+\ell^-$ and $\bar{B} \rightarrow \bar{K}\ell^+\ell^-$ decays into light leptons depend on a common combination of short-distance coefficients. The corresponding CP-asymmetries are hence identical. Furthermore we present low recoil predictions for $\bar{B} \rightarrow \bar{K}\ell^+\ell^-$ observables, including the flat term in the angular distribution which becomes sizable for taus. We work out model-independently the constraints on $\Delta B = 1$ operators using the most recent data from the experiments BaBar, Belle, CDF and LHCb. For constructive interference with the standard model, generic new physics is pushed up to scales above 44 TeV at 95% CL. Assuming none or small CP-violation we obtain a lower bound on the position of the zero of the forward-backward asymmetry of $\bar{B}^0 \rightarrow \bar{K}^{*0}\ell^+\ell^-$ decays as $q_0^2 > 1.7 \text{ GeV}^2$, which improves to $q_0^2 > 2.6 \text{ GeV}^2$ for a standard model-like sign $b \rightarrow s\gamma$ amplitude.

I. INTRODUCTION

Rare B -decays into dileptons are precision probes of the standard model (SM) and the flavor sector and provide constraints on physics beyond the standard model (BSM). Important semileptonic modes in terms of experimental accessibility and theory control are those into a K or a K^* . The latter decays exhibit a rich phenomenology especially through angular analysis of subsequent decays $\bar{B} \rightarrow \bar{K}^*(\rightarrow \bar{K}\pi)\ell^+\ell^-$, see [1] for a recent summary. Decays into a pseudo-scalar meson $\bar{B} \rightarrow \bar{K}\ell^+\ell^-$, $\ell = e, \mu, \tau$ allow to perform a number of complementary measurements as well. Observables include the decay rate Γ_ℓ , its CP-asymmetry A_{CP}^ℓ , the forward-backward asymmetry A_{FB}^ℓ and the flat term F_H^ℓ appearing in the angular distribution [2–4]

$$\frac{1}{\Gamma_\ell} \frac{d\Gamma_\ell}{d\cos\theta_\ell} = \frac{3}{4}(1 - F_H^\ell)(1 - \cos^2\theta_\ell) + \frac{1}{2}F_H^\ell + A_{\text{FB}}^\ell \cos\theta_\ell, \quad (1.1)$$

or distributions in the dilepton mass thereof. (The angle θ_ℓ is defined in Section II C.)

Previous systematic analyses of $\bar{B} \rightarrow \bar{K}\ell^+\ell^-$ distributions [4] focused on the region of large hadronic recoil, where QCD factorization (QCDF) applies [5, 6]. The intermediate recoil region where charmonium-resonances dominate the dilepton spectrum through $\bar{B} \rightarrow \bar{K}(J/\Psi, \Psi') \rightarrow \bar{K}\ell^+\ell^-$ decays has been studied recently [7]. In this work we provide a systematic analysis for the region of low hadronic recoil, that is, for large dilepton masses $\sqrt{q^2}$ of the order of the b -quark mass, above the Ψ' -peak.

The study of heavy-to-light decays at low recoil by means of a local operator product expansion (OPE) in $1/\sqrt{q^2}$ has been put forward by [8], and recently [9], see also [10] for earlier mention on inclusive decays. The simultaneous matching onto heavy quark effective theory (HQET) and use of the improved Isgur-Wise form factor relations [11] has been shown to be of benefit for $\bar{B} \rightarrow \bar{K}^*\ell^+\ell^-$ decays by allowing for the design of specific low recoil observables with sensitivity to either short- or long-distance physics as well as checks of the theory framework [12, 13]. Equally important, the theoretical accessibility of this kinematic region is necessary for a full exploitation of the available and future rare B -decay data. Note that roughly a similar amount of $\bar{B} \rightarrow \bar{K}^*\ell^+\ell^-$ data exists presently for the low and the large recoil region by all contemporary B -physics experiments, BaBar, Belle, CDF and LHCb. The latter will soon be competitive and eventually take over in statistics as indicated by the recent preliminary results on the angular distribution of $\bar{B}^0 \rightarrow \bar{K}^{*0}\ell^+\ell^-$ decays [14, 15]. As

for $\bar{B} \rightarrow \bar{K} \ell^+ \ell^-$ decays, LHCb reported so far 35 ± 7 events of $B^+ \rightarrow K^+ \mu^+ \mu^-$ within a recorded luminosity of 37pb^{-1} during the 2010 LHC run [16].

The plan of this paper is to work out and explore the phenomenology of $\bar{B} \rightarrow \bar{K} \ell^+ \ell^-$ decays at low hadronic recoil. We give in Section II the heavy-quark form factor relation, collect the expressions for the decay amplitude at low recoil and discuss the observables relevant to our model-independent framework. In Section III A we present SM predictions including a discussion of their uncertainties. In Section III B we derive constraints on the $\Delta B = 1$ short-distance couplings entering $\bar{B} \rightarrow \bar{K}^{(*)} \ell^+ \ell^-$ decays using the most recent experimental low and large recoil data. We conclude in Section IV. Details on the form factors are given in Appendix A.

II. THE DECAY $\bar{B} \rightarrow \bar{K} \ell^+ \ell^-$ AT LOW RECOIL

We use an effective $\Delta B = 1$ Hamiltonian to describe the flavor-changing $b \rightarrow s \ell^+ \ell^-$ transitions as

$$\begin{aligned} \mathcal{H}_{\text{eff}} = & -\frac{G_{\text{F}}}{\sqrt{2}} \frac{\alpha_e}{\pi} V_{tb} V_{ts}^* \\ & \times \left(\mathcal{C}_7 \frac{m_b}{e} [\bar{s} \sigma_{\mu\nu} P_R b] F^{\mu\nu} + \mathcal{C}_9 [\bar{s} \gamma_\mu P_L b] [\bar{\ell} \gamma^\mu \ell] + \mathcal{C}_{10} [\bar{s} \gamma_\mu P_L b] [\bar{\ell} \gamma^\mu \gamma_5 \ell] + \text{h.c.} \right) + \dots \end{aligned} \quad (2.1)$$

Here, the ellipses denote tree-level induced or subdominant contributions which we assume to be SM-like. Furthermore, V_{ij} denote CKM-elements and m_b the $\overline{\text{MS}}$ -mass of the b -quark. We allow the Wilson coefficients $\mathcal{C}_{7,9,10}$ to be complex-valued to account for CP-violation beyond the SM. We assume them throughout this work to be evaluated at the scale $\mu = m_b$. For further details we refer to previous low recoil works employing the same notation [12, 13].

A. The Improved Isgur-Wise Relation

The matrix elements of $\bar{B} \rightarrow \bar{K}$ transitions can be parameterized in terms of three q^2 -dependent form factors $f_{+,T,0}$ which are defined in Appendix A. Following [8, 11], the QCD operator identity

$$i \partial^\nu (\bar{s} i \sigma_{\mu\nu} b) = i \partial_\mu (\bar{s} b) - m_b (\bar{s} \gamma_\mu b) - 2 (\bar{s} i \overleftarrow{D}_\mu b) \quad (2.2)$$

allows to derive an improved Isgur-Wise relation between f_T and f_+ ,

$$f_T(q^2, \mu) = \frac{m_B(m_B + m_K)}{q^2} \left[\kappa(\mu) f_+(q^2) + \frac{2\delta_+^{(0)}(q^2)}{m_B} \right] + \mathcal{O}\left(\alpha_s \frac{\Lambda}{m_b}, \frac{\Lambda^2}{m_b^2}\right) \quad (2.3)$$

$$= \frac{m_B(m_B + m_K)}{q^2} \kappa(\mu) f_+(q^2) + \mathcal{O}\left(\frac{\Lambda}{m_b}\right), \quad (2.4)$$

in agreement with [17]. (We neglect the mass of the strange quark.) Here, we denote by m_B, m_K the B -meson and kaon mass, respectively, and neglect in the second line the subleading HQET form factor $\delta_+^{(0)}$, see Appendix A. The $1/q^2$ -factor on the right-hand side of Eqs. (2.3) and (2.4) is of kinematical origin, related to the definition of f_T , Eq. (A1). The μ -dependent coefficient κ reads, including $\mathcal{O}(\alpha_s)$ corrections, as

$$\kappa(\mu) = \left(1 + 2 \frac{D_0^{(v)}(\mu)}{C_0^{(v)}(\mu)} \right) \frac{m_b(\mu)}{m_B} \quad (2.5)$$

with the HQET Wilson coefficients $C_0^{(v)}, D_0^{(v)}$ given in [8]. At $\mu = m_b$ holds $\kappa = 1 + \mathcal{O}(\alpha_s^2)$. While deriving Eq. (2.4) one finds that the form factor f_0 is a power correction

$$f_0(q^2) = 0 + \mathcal{O}\left(\frac{\Lambda}{m_b}\right), \quad (2.6)$$

as expected from heavy quark symmetry [18].

B. The $\bar{B} \rightarrow \bar{K} \ell^+ \ell^-$ Matrix Element

Beyond the contributions from the operators in Eq. (2.1), the amplitude of $\bar{B} \rightarrow \bar{K} \ell^+ \ell^-$ also receives contributions from current-current and QCD-penguin operators. As a result of the OPE in $1/\sqrt{q^2}$ for the leading dimension 3-operators, these contributions can be taken into account by effective Wilson coefficients $\mathcal{C}_{7,9}^{\text{eff}}$ [9], whereas sub-leading contributions enter at dimension 5 and are suppressed by $(\Lambda/m_b)^2 \sim 2\%$. Here we follow [8] and subsequent low recoil $\bar{B} \rightarrow \bar{K}^* \ell^+ \ell^-$ works [12, 13] and perform an additional matching onto HQET and use the form factor relation Eq. (2.4). The effective coefficients are then given as [13]

$$\mathcal{C}_7^{\text{eff}} = \mathcal{C}_7 - \frac{1}{3} \left[\mathcal{C}_3 + \frac{4}{3} \mathcal{C}_4 + 20 \mathcal{C}_5 + \frac{80}{3} \mathcal{C}_6 \right] + \frac{\alpha_s}{4\pi} \left[(\mathcal{C}_1 - 6 \mathcal{C}_2) A(q^2) - \mathcal{C}_8 F_8^{(7)}(q^2) \right], \quad (2.7)$$

$$\begin{aligned} \mathcal{C}_9^{\text{eff}} &= \mathcal{C}_9 + h(0, q^2) \left[\frac{4}{3} \mathcal{C}_1 + \mathcal{C}_2 + \frac{11}{2} \mathcal{C}_3 - \frac{2}{3} \mathcal{C}_4 + 52 \mathcal{C}_5 - \frac{32}{3} \mathcal{C}_6 \right] \\ &\quad - \frac{1}{2} h(m_b, q^2) \left[7 \mathcal{C}_3 + \frac{4}{3} \mathcal{C}_4 + 76 \mathcal{C}_5 + \frac{64}{3} \mathcal{C}_6 \right] + \frac{4}{3} \left[\mathcal{C}_3 + \frac{16}{3} \mathcal{C}_5 + \frac{16}{9} \mathcal{C}_6 \right] \end{aligned} \quad (2.8)$$

$$\begin{aligned}
& + \frac{\alpha_s}{4\pi} \left[\mathcal{C}_1 (B(q^2) + 4C(q^2)) - 3\mathcal{C}_2 (2B(q^2) - C(q^2)) - \mathcal{C}_8 F_8^{(9)}(q^2) \right] \\
& + 8 \frac{m_c^2}{q^2} \left[\left(\frac{4}{9} \mathcal{C}_1 + \frac{1}{3} \mathcal{C}_2 \right) (1 + \hat{\lambda}_u) + 2\mathcal{C}_3 + 20\mathcal{C}_5 \right].
\end{aligned}$$

These include the NLO QCD matching corrections and doubly Cabibbo-suppressed contributions proportional to $\lambda_u = V_{ub}V_{us}^*/(V_{tb}V_{ts}^*)$. The latter are responsible for the tiny amount of CP-violation in the SM in $b \rightarrow s$ transitions.

The $\bar{B} \rightarrow \bar{K} \ell^+ \ell^-$ decay amplitude [4] simplifies within the SM operator basis Eq. (2.1) after applying the form factor relation Eq. (2.4) to

$$\mathcal{A}(\bar{B} \rightarrow \bar{K} \ell^+ \ell^-) = i \frac{G_F \alpha_e}{\sqrt{2}\pi} V_{tb} V_{ts}^* f_+(q^2) [F_V p^\mu (\bar{\ell} \gamma_\mu \ell) + F_A p^\mu (\bar{\ell} \gamma_\mu \gamma_5 \ell) + F_P (\bar{\ell} \gamma_5 \ell)], \quad (2.9)$$

where

$$\begin{aligned}
F_A &= \mathcal{C}_{10}, & F_V &= \mathcal{C}_9^{\text{eff}} + \kappa \frac{2m_b m_B}{q^2} \mathcal{C}_7^{\text{eff}}, \\
F_P &= -m_\ell \left[1 + \frac{m_B^2 - m_K^2}{q^2} \left(1 - \frac{f_0}{f_+} \right) \right] \mathcal{C}_{10},
\end{aligned} \quad (2.10)$$

and p^μ denotes the 4-momentum of the B -meson and m_ℓ the lepton mass.

The use of Eq. (2.4) introduces an uncertainty of $\mathcal{O}(\Lambda/m_b)$ in the term proportional to $\mathcal{C}_7^{\text{eff}}$ in F_V , however, the phenomenological impact of this uncertainty is additionally suppressed by $\mathcal{C}_7^{\text{eff}}/\mathcal{C}_9^{\text{eff}}$, which is ~ 0.1 in the SM. Further subleading $1/m_b$ contributions to the amplitude F_V in Eq. (2.9) itself receive an additional suppression of α_s [8]. The associated uncertainties are included in our phenomenological analysis following the procedure described in [13].

The coefficient F_P is suppressed by m_ℓ/m_B and hence small for light leptons. Since the form factor f_0 enters F_P only, its impact for phenomenological implications is negligible except for taus.

C. Observables and Angular Distribution

Continuing along the lines of [4], we write the differential $\bar{B} \rightarrow \bar{K} \ell^+ \ell^-$ decay distributions as

$$\frac{d^2\Gamma_\ell[\bar{B} \rightarrow \bar{K} \ell^+ \ell^-]}{dq^2 d\cos\theta_\ell} = a_\ell(q^2) + b_\ell(q^2) \cos\theta_\ell + c_\ell(q^2) \cos^2\theta_\ell, \quad (2.11)$$

$$\frac{d\Gamma_\ell[\bar{B} \rightarrow \bar{K} \ell^+ \ell^-]}{dq^2} = 2 \left[a_\ell(q^2) + \frac{1}{3} c_\ell(q^2) \right] \quad (2.12)$$

with q^2 -dependent observables a_ℓ , b_ℓ and c_ℓ . The angle θ_ℓ is defined as the angle between the \bar{B} -direction and the ℓ^- -direction in the $\ell^+\ell^-$ rest frame. Within the SM operator basis Eq. (2.1)

$$\begin{aligned} \frac{a_\ell}{\Gamma_0 \sqrt{\lambda} \beta_\ell f_+^2} &= \frac{\lambda}{4} (|F_A|^2 + |F_V|^2) \\ &\quad + 2m_\ell(m_B^2 - m_K^2 + q^2) \text{Re}(F_P F_A^*) + 4m_\ell^2 m_B^2 |F_A|^2 + q^2 |F_P|^2, \\ b_\ell &= 0, \\ \frac{c_\ell}{\Gamma_0 \sqrt{\lambda} \beta_\ell f_+^2} &= -\beta_\ell^2 \frac{\lambda}{4} (|F_A|^2 + |F_V|^2) \end{aligned} \quad (2.13)$$

with

$$\Gamma_0 = \frac{G_F^2 \alpha_e^2 |V_{tb} V_{ts}^*|^2}{2^9 \pi^5 m_B^3}, \quad \beta_\ell = \sqrt{1 - \frac{4m_\ell^2}{q^2}}, \quad (2.14)$$

$$\lambda \equiv \lambda(m_B^2, m_K^2, q^2) = m_B^4 + m_K^4 + q^4 - 2(m_B^2 m_K^2 + m_B^2 q^2 + m_K^2 q^2).$$

The terms in the $\bar{B} \rightarrow \bar{K} \ell^+ \ell^-$ angular distribution Eq. (1.1) can then be obtained as [4]

$$\Gamma_\ell = 2 \int_{q_{\min}^2}^{q_{\max}^2} dq^2 (a_\ell + \frac{1}{3} c_\ell), \quad (2.15)$$

$$A_{\text{FB}}^\ell = 0, \quad (2.16)$$

$$F_H^\ell = \frac{2}{\Gamma_\ell} \int_{q_{\min}^2}^{q_{\max}^2} dq^2 (a_\ell + c_\ell). \quad (2.17)$$

The forward-backward asymmetry of $\bar{B} \rightarrow \bar{K} \ell^+ \ell^-$ decays is zero within the SM operator basis¹ and F_H^ℓ is suppressed by lepton mass, see below. However both observables receive contributions from scalar and tensor operators, and can signal such BSM effects [4, 20].

For $\ell = e, \mu$ we can safely neglect the lepton mass. In this limit $\beta_\ell = 1$ and

$$a_\ell = \Gamma_0 \frac{\sqrt{\lambda}^3}{4} f_+^2 \rho_1, \quad c_\ell = -a_\ell, \quad (2.18)$$

with the short-distance coefficient

$$\rho_1 = \left| \mathcal{C}_9^{\text{eff}} + \kappa \frac{2m_b m_B}{q^2} \mathcal{C}_7^{\text{eff}} \right|^2 + |\mathcal{C}_{10}|^2. \quad (2.19)$$

¹ Non-zero values in the SM originate from QED corrections and are tiny [4, 19].

The differential decay rate at low recoil can then be written as

$$\frac{d\Gamma_\ell[\bar{B} \rightarrow \bar{K}\ell^+\ell^-]}{dq^2} = \Gamma_0 \frac{\sqrt{\lambda}^3}{3} f_+^2 \rho_1, \quad (2.20)$$

and F_H^ℓ vanishes for $m_\ell = 0$.

The SM value of ρ_1 and its associated uncertainties have been presented earlier in the discussion of $\bar{B} \rightarrow \bar{K}^*\ell^+\ell^-$ decays at low recoil [12]. The appearance of the same short-distance factor ρ_1 in both vector and pseudoscalar final states uniquely correlates the decays $\bar{B} \rightarrow \bar{K}\ell^+\ell^-$ and $\bar{B} \rightarrow \bar{K}^*\ell^+\ell^-$ into light leptons. As a consequence, the CP-asymmetry of the decay rate, A_{CP}^ℓ , is identical

$$\begin{aligned} A_{\text{CP}}^\ell[\bar{B} \rightarrow \bar{K}\ell^+\ell^-] &= \frac{d\Gamma_\ell[\bar{B} \rightarrow \bar{K}\ell^+\ell^-]/dq^2 - d\Gamma_\ell[B \rightarrow K\ell^+\ell^-]/dq^2}{d\Gamma_\ell[\bar{B} \rightarrow \bar{K}\ell^+\ell^-]/dq^2 + d\Gamma_\ell[B \rightarrow K\ell^+\ell^-]/dq^2} \\ &= \frac{\rho_1 - \bar{\rho}_1}{\rho_1 + \bar{\rho}_1} = a_{\text{CP}}^{(1)}[\bar{B} \rightarrow \bar{K}^*\ell^+\ell^-], \end{aligned} \quad (2.21)$$

where $\bar{\rho}_1$ is obtained from ρ_1 by complex conjugation of the weak phases, *i.e.*, the CKM matrix elements and the Wilson coefficients \mathcal{C}_i . The CP-asymmetry $a_{\text{CP}}^{(1)}$ is form factor-free and essentially vanishes in the SM $|a_{\text{CP}}^{(1)}|_{\text{SM}} \lesssim 10^{-4}$ [13].

Keeping the lepton mass finite we obtain

$$a_\ell = \frac{\Gamma_0}{4} \sqrt{\lambda}^3 \beta_\ell f_+^2 \left[\rho_1 - \frac{4m_\ell^2}{q^2} |\mathcal{C}_{10}|^2 \mathcal{F}_0 \right], \quad c_\ell = -\frac{\Gamma_0}{4} \sqrt{\lambda}^3 \beta_\ell^3 f_+^2 \rho_1, \quad (2.22)$$

with

$$\mathcal{F}_0 = 1 - \frac{(m_B^2 - m_K^2)^2}{\lambda} \left(\frac{f_0}{f_+} \right)^2. \quad (2.23)$$

The second term in \mathcal{F}_0 is order one despite f_0 being a power correction, see Eq. (2.6), because of the phase space enhancement by the factor $\lambda \sim \mathcal{O}(\Lambda^2 m_B^2)$ in the denominator.

The q^2 -differential flat term of the angular distribution

$$F_H^\ell(q^2) = \frac{a_\ell + c_\ell}{a_\ell + \frac{1}{3}c_\ell} = \frac{6m_\ell^2}{q^2} \times \frac{\rho_1 - |\mathcal{C}_{10}|^2 \mathcal{F}_0}{\rho_1 + \frac{2m_\ell^2}{q^2} (\rho_1 - 3|\mathcal{C}_{10}|^2 \mathcal{F}_0)} \quad (2.24)$$

can be sizable for $\ell = \tau$, as we show explicitly in Section III A for the SM. The $F_H^\tau(q^2)$ -observable is complementary to the $\bar{B} \rightarrow \bar{K}\ell^+\ell^-$ branching ratios. From combined analysis with the branching ratios of $\bar{B} \rightarrow \bar{K}^{(*)}\ell^+\ell^-$ for $\ell = e, \mu$ decays the coefficient ρ_1 could be extracted together with the magnitude of \mathcal{C}_{10} , see also [21], given sufficient control of f_0/f_+ .

A	$0.812_{-0.027}^{+0.013}$	[23]	λ	0.22543 ± 0.00077	[23]
$\bar{\rho}$	0.144 ± 0.025	[23]	$\bar{\eta}$	$0.342_{-0.015}^{+0.016}$	[23]
$\alpha_s(M_Z)$	0.11762		τ_{B^+}	1.638 ps	[24]
$\alpha_e(m_b)$	1/133		τ_{B^0}	1.525 ps	[24]
$m_c(m_c)$	$(1.27_{-0.09}^{+0.07})$ GeV	[24]	m_{B^+}	5.2792 GeV	[24]
$m_b(m_b)$	$(4.19_{-0.06}^{+0.18})$ GeV	[24]	m_{B^0}	5.2795 GeV	[24]
m_t^{pole}	(173.3 ± 1.3) GeV	[25]	m_{K^+}	0.494 GeV	[24]
m_e	0.511 MeV	[24]	m_{K^0}	0.498 GeV	[24]
m_μ	0.106 GeV	[24]	M_W	(80.399 ± 0.023) GeV	[24]
m_τ	1.777 GeV	[24]	$\sin^2 \theta_W$	0.23116 ± 0.00013	[24]

TABLE I. The numerical input used in our analysis. We neglect the mass of the strange quark. The superscript $^0(^+)$ refers to neutral (charged) parameters.

III. PHENOMENOLOGICAL ANALYSIS

For the phenomenological analysis of the various rare B decay observables we use the numerical inputs given in Table I. All numerical results presented are obtained with the EOS flavor tool [22]. All experimental $\bar{B} \rightarrow \bar{K}^{(*)}\ell^+\ell^-$ results shown and used are CP-averages, and should silently be understood as those.

A. Standard Model Predictions for $\bar{B} \rightarrow \bar{K}\ell^+\ell^-$

The SM predictions for the $\bar{B} \rightarrow \bar{K}\ell^+\ell^-$ observables at low recoil in the framework described in Section II are given in Table II. The integration region is $14.18 \text{ GeV}^2 \leq q^2 \leq (m_B - m_K)^2$, *i.e.*, above the Ψ' -resonance. We employ the form factors f_+ and f_0 – the latter is required for decays to massive leptons only – from light cone QCD sum rule (LCSR) calculations and a q^2 -shape by a series expansion from [7] extrapolated to high q^2 . Our choice is motivated by the good agreement with preliminary unquenched lattice results [26] and the availability of uncertainties for the parameterization of the form factors, see Appendix A for details. The dependence on the tensor form factor has been removed by means of Eq. (2.4).

The uncertainties given in Table II originate from the form factors (FF), specifically the variation of the inputs Table IV to the parameterization Eq. (A3), the CKM matrix elements

Observable	Central Value	FF	SD	SL	CKM
$10^7 \times \mathcal{B}(B^- \rightarrow K^- \ell^+ \ell^-)$	1.04	+0.60 -0.27	+0.04 -0.02	+0.03 -0.03	+0.04 -0.07
$10^7 \times \mathcal{B}(B^- \rightarrow K^- \tau^+ \tau^-)$	1.26	+0.40 -0.21	+0.04 -0.03	+0.02 -0.02	+0.05 -0.09
$10^3 \times F_H^\mu$	7.50	+2.85 -2.61	+0.04 -0.10	+0.10 -0.10	-
$10^1 \times F_H^\tau$	8.90	+0.33 -0.45	+0.01 -0.02	+0.02 -0.02	-

TABLE II. The SM branching ratios and flat terms F_H^ℓ Eq. (2.17) integrated from 14.18 GeV² to $(m_B - m_K)^2$. For a description of the uncertainties see text. The branching ratios for the light leptons $\ell = e$ and $\ell = \mu$ are equal within the given precision (finite lepton masses are taken into account). The branching ratios for neutral B decays are obtained by rescaling the corresponding charged ones with τ_{B^0}/τ_{B^+} . All branching ratios are identical within the given accuracy to the ones of the corresponding CP-conjugated decays.

(CKM), and the short-distance parameters m_t^{pole} , M_W , $\sin^2 \theta_W$ as well as the scale μ varied within $[\mu_b/2, 2\mu_b]$ with $\mu_b = 4.2$ GeV collectively denoted as (SD). We evaluate the SM Wilson coefficients at next-to-next-to-leading order. In addition, we take into account the (unknown) subleading $1/m_b$ -corrections to the $\bar{B} \rightarrow \bar{K} \ell^+ \ell^-$ matrix elements and form factor relation Eq. (2.4) (SL). The latter uncertainty is estimated with the procedure outlined in the Appendix of [13] adopted to $\bar{B} \rightarrow \bar{K} \ell^+ \ell^-$ decays. The residual CKM uncertainty from $\hat{\lambda}_u$ in F_H^ℓ has been dropped in Table II because it is below the given precision. To the accuracy given in Table II SM CP-violation is too small to induce any effect.

At high q^2 weak annihilation topologies are strongly suppressed by $(\Lambda/m_b)^3$ [9], and thus isospin breaking effects are dominated by the differences in the lifetime. The branching ratios of decays of neutral B -mesons are obtained by rescaling the corresponding branching ratios of charged B decays in Table II with the ratio of lifetimes τ_{B^0}/τ_{B^+} . In the numerics we keep as well the very small effect of isospin breaking by the masses m_B and m_K .

We show the SM predictions for $d\mathcal{B}(B^- \rightarrow K^- \mu^+ \mu^-)/dq^2$ in Fig. 1 versus existing data² by Belle [27] (red points), CDF [28] (black points) and BaBar [3] (orange points) and with individual uncertainty budgets in Fig. 2. In Fig. 3 we show the differential SM branching

² The data on the binned $\bar{B} \rightarrow \bar{K} \ell^+ \ell^-$ branching ratios by Belle and BaBar are publicly available for an unknown admixture of charged and neutral B decays only. We find differences of the order of the scan resolution in the constraints Figs. 5 and 6 when interpreting the Belle data as either purely charged or as purely neutral B decays. This effect will be even less important in the future with improved statistics.

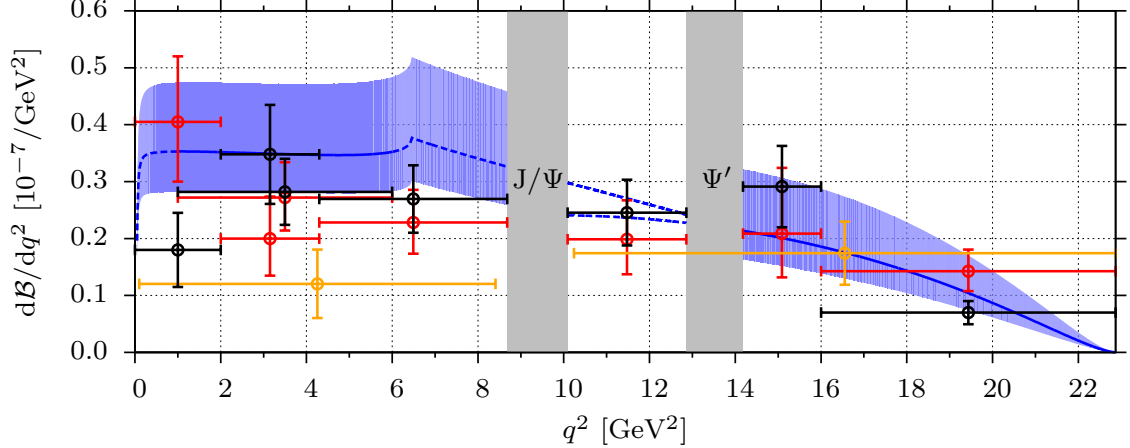


FIG. 1. The SM branching ratio $d\mathcal{B}(B^- \rightarrow K^- \mu^+ \mu^-)/dq^2$ using form factors from [7] (blue solid and dashed lines) alongside the measurements by Belle [27] (red points), CDF [28] (black points) and BaBar [3] (orange points), see footnote 2. The blue band shows the theoretical uncertainties described in the text added in quadrature. The vertical (grey) bands are the experimental veto regions [27, 28] to remove contributions from $\bar{B} \rightarrow J/\Psi(\rightarrow \mu^+ \mu^-) \bar{K}$ (left-hand band) and $\bar{B} \rightarrow \Psi'(\rightarrow \mu^+ \mu^-) \bar{K}$ (right-hand band). The dashed (blue) lines below the J/Ψ (between the charmonium bands) correspond to theory extrapolations from the low recoil (low and large recoil) region.

ratio into ditaus. The evaluation of observables in the large recoil region is carried out within the framework of QCDF [5, 6]. We employ the same $\bar{B} \rightarrow \bar{K} \ell^+ \ell^-$ form factors used at low recoil, *i.e.*, the ones from Ref. [7]. The treatment of the subleading corrections for low q^2 is adapted from [29]. The flat term $F_H^\ell(q^2)$ for both muons and taus is shown in Fig. 4. The growth of $F_H^\mu(q^2)$ at both ends of the spectrum results from a finite muon mass. While at low q^2 such effects are kinematically enhanced by m_μ^2/q^2 , the effect at the very high q^2 -end is induced by the vanishing decay rate in the denominator. For electrons these effects are further suppressed by $m_e^2/m_\mu^2 \sim 10^{-5}$, and negligible.

B. Model-Independent Analysis

We perform a model-independent analysis in the $\Delta B = 1$ complex-valued Wilson coefficients $\mathcal{C}_k = |\mathcal{C}_k| \exp(i\phi_k)$, $k = 7, 9, 10$. We build on the analysis by [12, 13] using the updated data from CDF [28, 31], the first $\bar{B} \rightarrow \bar{K}^* \mu^+ \mu^-$ data from LHCb [14, 15], and include $\bar{B} \rightarrow \bar{K} \ell^+ \ell^-$

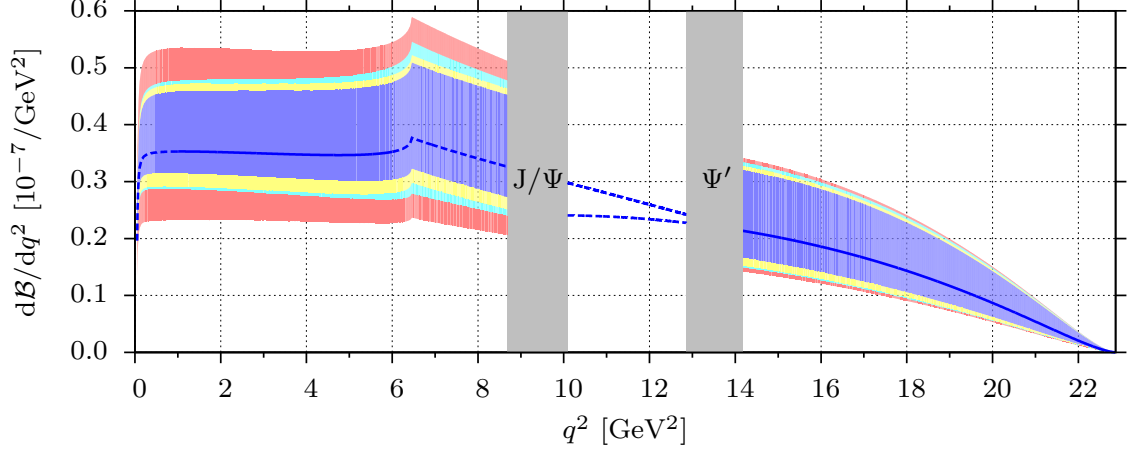


FIG. 2. The SM branching ratio $d\mathcal{B}(B^- \rightarrow K^- \mu^+ \mu^-)/dq^2$ with the linearly added uncertainties from the form factors (blue), the CKM matrix elements (yellow), the short-distance input (cyan) and the subleading $1/m_b$ corrections (red), see also Fig. 1.

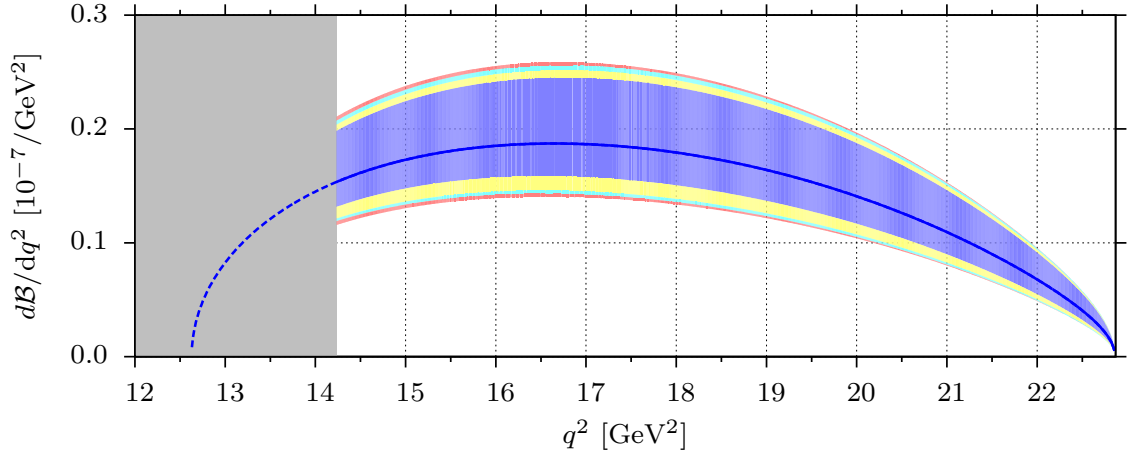


FIG. 3. The SM branching ratio $d\mathcal{B}(B^- \rightarrow K^- \tau^+ \tau^-)/dq^2$ with linearly added uncertainties, see Fig. 2. The grey band refers to the cut from BaBar's search for this channel [30].

decays. The corresponding experimental results for the latter branching ratios from Belle [27] and CDF [28] are given in Table III, and also shown in Fig. 1 (see also footnote 2). The data by BaBar [3] shown as well in Fig. 1 are not used as none of the two bins are fully applicable to low- or high- q^2 theory frameworks. We discard CDF's data on $\mathcal{B}(\bar{B}^0 \rightarrow \bar{K}^0 \mu^+ \mu^-)$ [28] as the uncertainties are very large. First, binned measurements of A_{FB}^ℓ for light leptons are available and are consistent with $A_{\text{FB}}^\ell = 0$ [27, 31]. These data are not taken into account because within the context of the SM operator basis used in this analysis A_{FB}^ℓ vanishes, see

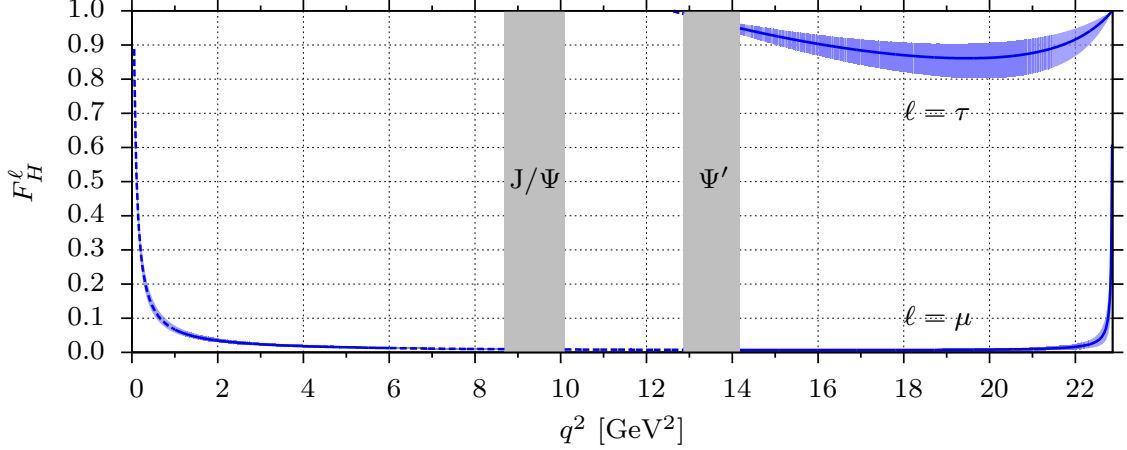


FIG. 4. The flat term $F_H^\ell(q^2)$ for $B^- \rightarrow K^- \ell^+ \ell^-$ decays given in Eq. (2.24) for $\ell = \mu$ (lower curve) and $\ell = \tau$ (upper band) in the SM. The theoretical uncertainties are added in quadrature.

Observable	SM Prediction	Measurement
$\mathcal{B}(\bar{B}^0 \rightarrow \bar{K}^0 \mu^+ \mu^-)_{1.0,6.0}$	$(1.59_{-0.35}^{+0.59}) \times 10^{-7}$ * [4]	$(1.36_{-0.29}^{+0.31}) \times 10^{-7}$ † [27]
$\mathcal{B}(B^- \rightarrow K^- \mu^+ \mu^-)_{1.0,6.0}$	$(1.75_{-0.38}^{+0.64}) \times 10^{-7}$ * [4]	$(1.41_{-0.29}^{+0.29}) \times 10^{-7}$ [28]
$\mathcal{B}(\bar{B}^0 \rightarrow \bar{K}^0 \mu^+ \mu^-)_{14.18,16.00}$	$(0.34_{-0.09}^{+0.18}) \times 10^{-7}$	$(0.38_{-0.14}^{+0.21}) \times 10^{-7}$ † [27]
$\mathcal{B}(B^- \rightarrow K^- \mu^+ \mu^-)_{14.18,16.00}$	$(0.37_{-0.09}^{+0.20}) \times 10^{-7}$	$(0.53_{-0.13}^{+0.13}) \times 10^{-7}$ [28]
$\mathcal{B}(\bar{B}^0 \rightarrow \bar{K}^0 \mu^+ \mu^-)_{16.00,22.86}$	$(0.63_{-0.18}^{+0.39}) \times 10^{-7}$	$(0.98_{-0.24}^{+0.26}) \times 10^{-7}$ † [27]
$\mathcal{B}(B^- \rightarrow K^- \mu^+ \mu^-)_{16.00,22.90}$	$(0.68_{-0.19}^{+0.41}) \times 10^{-7}$	$(0.48_{-0.14}^{+0.14}) \times 10^{-7}$ [28]

TABLE III. The $\bar{B} \rightarrow \bar{K} \ell^+ \ell^-$ branching ratios and their respective measurements with systematic and statistical uncertainties added linearly by Belle [27] and CDF [28] used to constrain $\mathcal{C}_{7,9,10}$. All entries are understood as CP-averaged. The integration binning $q_{\min}^2 \leq q^2 < q_{\max}^2$ in GeV^2 is indicated as $\mathcal{B}_{q_{\min}^2, q_{\max}^2}$. *Includes updates to the numerical input and uses a different parametrization of the form factors than [4]. †see footnote 2.

Eq. (2.16). Decays into ditaus have not been observed. The presently best limit stems from BaBar $\mathcal{B}(B^+ \rightarrow K^+ \tau^+ \tau^-) < 3.3 \times 10^{-3}$ for $q^2 > 14.23 \text{ GeV}^2$ at 90% CL [30].

We perform a six-dimensional parameter scan over the magnitudes $|\mathcal{C}_{7,9,10}|$ and weak phases $\phi_{7,9,10}$. The resolution in $|\mathcal{C}_{9,10}|$ is 0.25, and $\pi/16$ in $\phi_{7,9,10}$. We vary $0.3 < |\mathcal{C}_7| \leq 0.4$ with step-width 0.02. Statistical and systematic experimental uncertainties are added linearly in the scan. Contrary to [13] we do not symmetrize the uncertainties, however, we checked

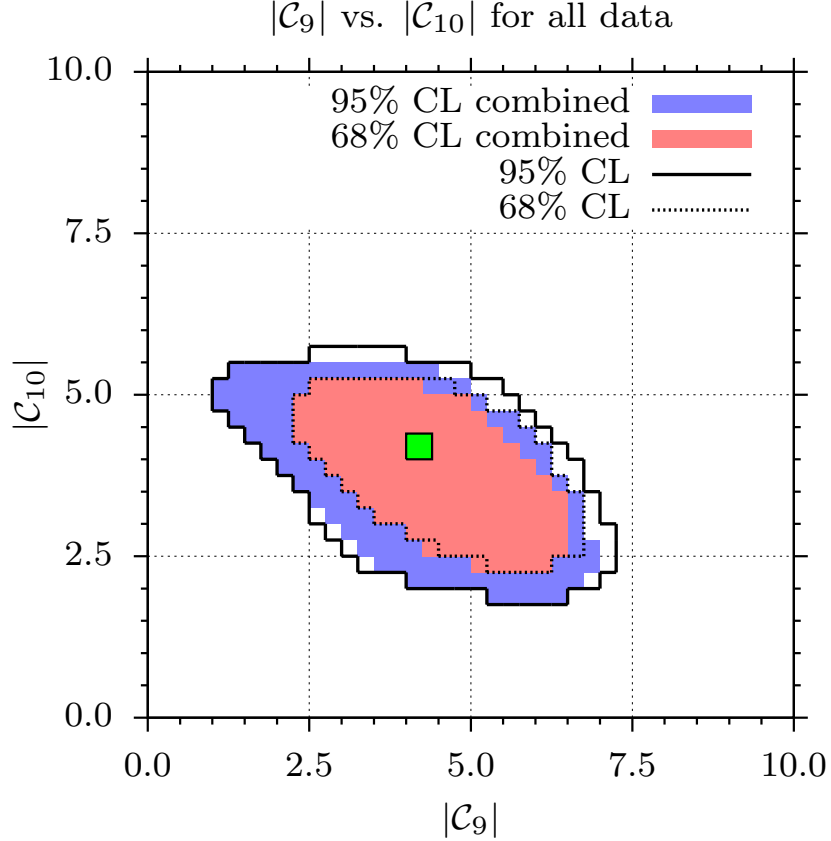


FIG. 5. Constraints on $|\mathcal{C}_9|$ and $|\mathcal{C}_{10}|$ from the combined analysis of $\bar{B} \rightarrow \{\bar{K}, \bar{K}^*, X_s\} \ell^+ \ell^-$ decays at 68% CL (red area) and 95% CL (blue area). The 68% CL (dotted) and 95% CL (solid) contours without using $\bar{B} \rightarrow \bar{K} \ell^+ \ell^-$ decays are shown as well. The green square marks the SM prediction.

that with the current data the results exhibit insignificant differences only between using symmetrized and un-symmetrized uncertainties. The constraints on $|\mathcal{C}_9|$ - $|\mathcal{C}_{10}|$ from the joint $\bar{B} \rightarrow \bar{K}^* \ell^+ \ell^-$, $\bar{B} \rightarrow \bar{K} \ell^+ \ell^-$ and $\bar{B} \rightarrow X_s \ell^+ \ell^-$ analysis are presented in Fig. 5. The inner (outer) colored areas are allowed at 68% CL (95% CL). The inclusion of the decay $\bar{B} \rightarrow \bar{K} \ell^+ \ell^-$ improves the scan, as can be seen from the overlaid contours obtained without using $\bar{B} \rightarrow \bar{K} \ell^+ \ell^-$ data. As the latter enter the analysis only via branching ratios, they put constraints on ρ_1 , roughly $\sim |\mathcal{C}_9|^2 + |\mathcal{C}_{10}|^2$, and show very little sensitivity to CP phases [32]. In Fig. 6 we show the constraints from $\bar{B} \rightarrow \bar{K} \ell^+ \ell^-$ decays alone in the large recoil region, the low recoil region and for both kinematic regions, respectively. All these constraints are consistent with each other and the agreement with the SM is good.

From the full scan we obtain the allowed ranges

$$2.3 \leq |\mathcal{C}_9| \leq 6.5, \quad (1.0 \leq |\mathcal{C}_9| \leq 7.0), \quad (3.1)$$

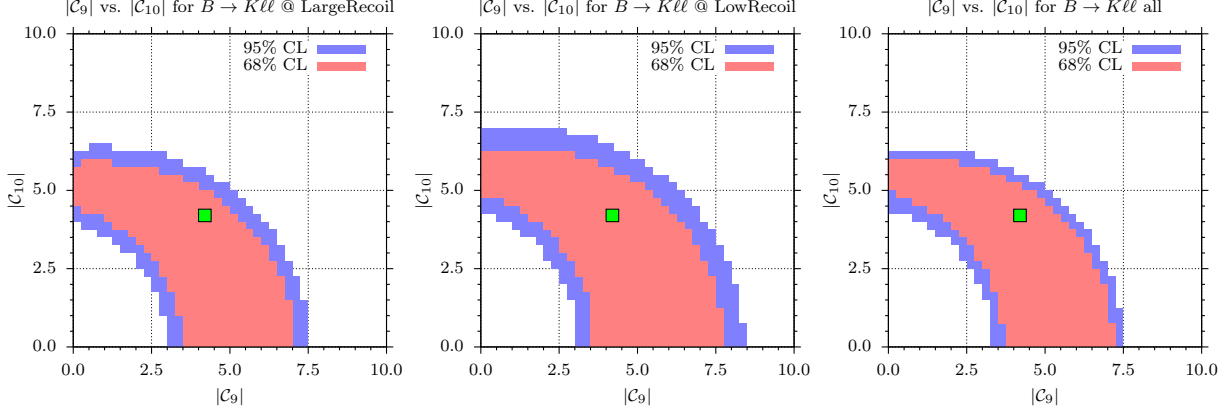


FIG. 6. The constraints from $\bar{B} \rightarrow \bar{K} \ell^+ \ell^-$ decays on $|\mathcal{C}_9|$ and $|\mathcal{C}_{10}|$ from the large-recoil region (left-hand plot), the low-recoil region (plot in the middle) and both (right-hand plot), for further notation see Fig. 5.

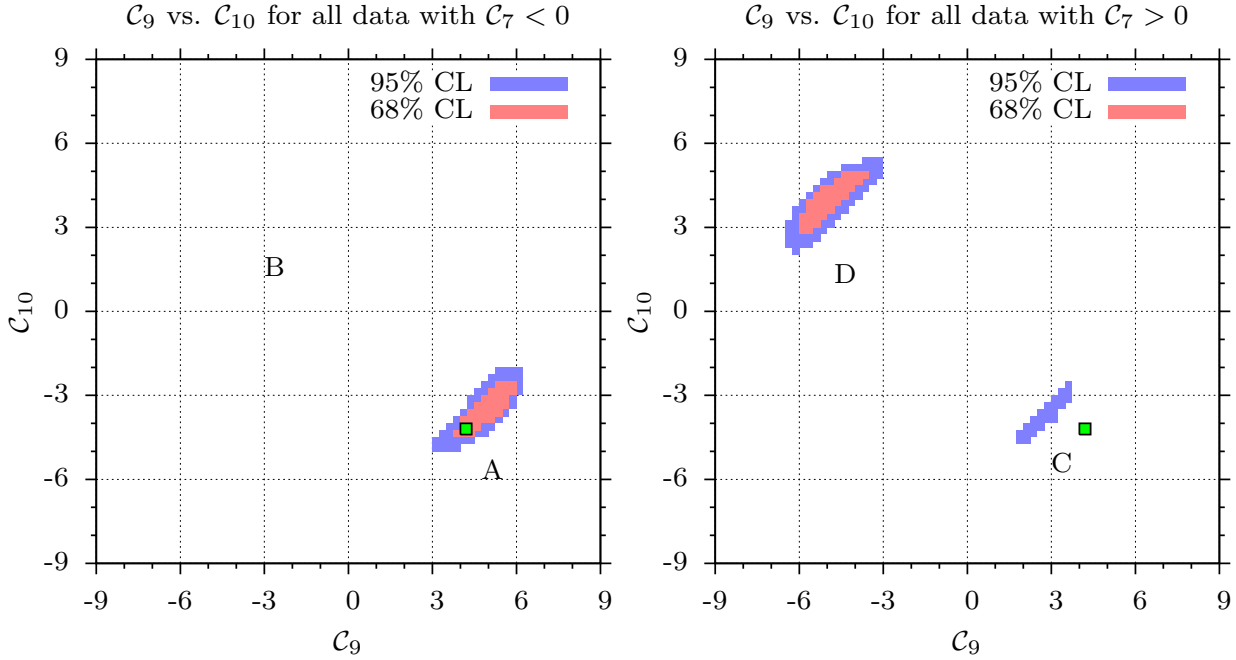


FIG. 7. The constraints from all the currently available data on the real-valued Wilson coefficients \mathcal{C}_9 and \mathcal{C}_{10} for SM-like sign $\mathcal{C}_7 < 0$ (left-hand plot) and $\mathcal{C}_7 > 0$ (right-hand plot), for further notation see Fig. 5.

$$2.3 \leq |\mathcal{C}_{10}| \leq 5.3, \quad (1.8 \leq |\mathcal{C}_{10}| \leq 5.5) \quad (3.2)$$

at 68% CL (95% CL), see Fig. 5. This implies that the branching ratios $\mathcal{B}(\bar{B}_s \rightarrow \ell^+ \ell^-) \propto |\mathcal{C}_{10}|^2$ for $\ell = e, \mu, \tau$ can be enhanced by at most a factor of 1.7 at 95% CL with respect to

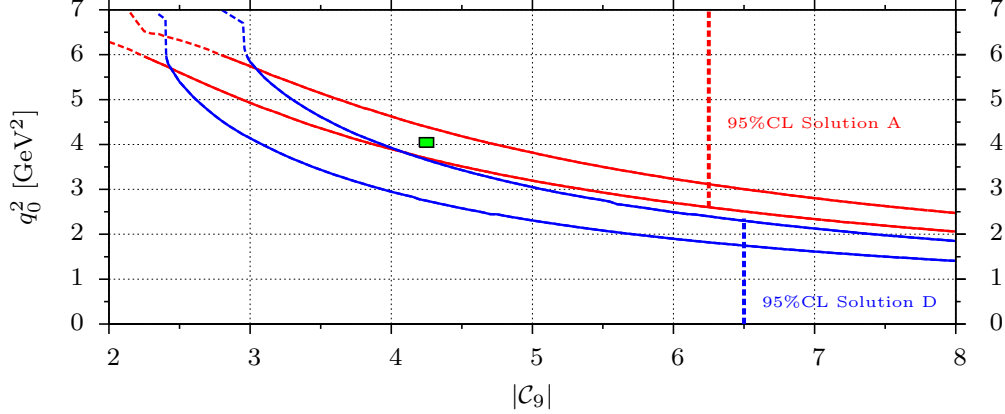


FIG. 8. The zero of the forward-backward asymmetry q_0^2 in $\bar{B}^0 \rightarrow \bar{K}^{*0}\ell^+\ell^-$ decays at 1σ versus $|\mathcal{C}_9|$ for $\mathcal{C}_7 < 0$ (solution A in Fig. 7, red lines) and $\mathcal{C}_7 > 0$ (solution D in Fig. 7, blue lines) assuming no BSM CP-violation. The vertical lines denote the corresponding 95% CL upper limits on $|\mathcal{C}_9|$ from Fig. 7. The green area marks the SM (for fixed $\mu = 4.2$ GeV).

their SM value.

Furthermore, we obtain constraints for real-valued Wilson coefficients $\mathcal{C}_{9,10}$ by discarding from the complex-valued scan all data with $\phi_{7,9,10} \neq 0, \pi$. These constraints are shown in Fig. 7. A previously existing region, labelled B, is now excluded, while region C is disfavored at 95% CL. With CP-violation neglected the upper bound on $|\mathcal{C}_9|$ provides a lower limit on the zero crossing q_0^2 of the forward-backward asymmetry in $\bar{B} \rightarrow \bar{K}^*\ell^+\ell^-$ decays [33]. We find $q_0^2 > 1.7$ GeV², which gets improved to $q_0^2 > 2.6$ GeV² assuming the sign of \mathcal{C}_7 to be SM-like, that is, negative. The zero as a function of $|\mathcal{C}_9|$ (for fixed $\mu = 4.2$ GeV) for $\bar{B}^0 \rightarrow \bar{K}^{*0}\mu^+\mu^-$ decays is shown in Fig. 8 for both sign combinations which allow for a zero, that is, solution A and D of Fig. 7. There is no such limit on q_0^2 in the fully CP-violating case. The dashed curves denote extrapolations to $q^2 \gtrsim 6$ GeV² where QCDF may not be applicable.

In the SM we find the zero to be located at

$$q_0^{2,\text{SM}} = \left(3.97_{-0.03}^{+0.03} \Big|_{\text{FF}} \begin{matrix} +0.09 \\ -0.09 \end{matrix} \Big|_{\text{SL}} \begin{matrix} +0.29 \\ -0.27 \end{matrix} \Big|_{\text{SD}} \right) \text{ GeV}^2 \quad (3.3)$$

consistent with [6, 29, 34]. The SD uncertainty without the one from the scale μ is ${}_{-0.05}^{+0.16}$ GeV². The location of the zero is form factor-independent only at lowest order in $1/m_b$ [2, 5]. The uncertainty denoted by FF stems from varying the LCSR inputs to the form factors used in the scan to describe $\bar{B} \rightarrow \bar{K}^*\ell^+\ell^-$ decays by [35].

One can ask about the implications for generic new physics from the $\Delta B = 1$ BSM operators $\sum_i \frac{\tilde{c}_i}{\Lambda_{\text{NP}}^2} \tilde{O}_i$, where

$$\tilde{O}_9 = \bar{s}\gamma_\mu(1 - \gamma_5)b\bar{\mu}\gamma^\mu\mu, \quad \tilde{O}_{10} = \bar{s}\gamma_\mu(1 - \gamma_5)b\bar{\mu}\gamma^\mu\gamma_5\mu. \quad (3.4)$$

Assuming unsuppressed contributions, $|\tilde{c}_{9,10}| = 1$, the scale of new physics Λ_{NP} must be as high as

$$\Lambda_{\text{NP}} > 30 \text{ TeV (15 TeV)} \quad \text{from } \tilde{O}_9, \quad (3.5)$$

$$\Lambda_{\text{NP}} > 44 \text{ TeV (16 TeV)} \quad \text{from } \tilde{O}_{10}. \quad (3.6)$$

On the other hand, with $\Lambda_{\text{NP}} = 1 \text{ TeV}$ the coefficient of the higher dimensional operator \tilde{O}_{10} needs a (flavor) suppression as strong as $|\tilde{c}_{10}| < 5 \times 10^{-4}$ (4×10^{-3}). The corresponding numbers for \tilde{O}_9 read $|\tilde{c}_9| < 1 \times 10^{-3}$ (5×10^{-3}). The bounds are obtained at 95% CL from Eqs. (3.1) and (3.2). For all cases the first (second) number corresponds to constructive (destructive) interference with the SM. The bounds from \mathcal{C}_{10} are stronger than those of \mathcal{C}_9 .

IV. CONCLUSION

With event samples of order several hundred analyzed [3, 14, 15, 27, 28] and beyond a thousand from LHCb alone at the horizon [16] the studies of rare decays $\bar{B} \rightarrow \bar{K}^{(*)}\ell^+\ell^-$ begin to reach deep into the space of $\Delta B = 1$ weak operators in terms of the allowed ranges and correlations of the short-distance couplings.

Allowing for BSM CP-violation the current status is shown in Fig. 5, updating the analysis of [13] for the moduli of the Wilson coefficients \mathcal{C}_9 and \mathcal{C}_{10} by including the data from LHCb [14] and $\bar{B} \rightarrow \bar{K}\ell^+\ell^-$ decays. For the latter we worked out predictions for the kinematic region of low hadronic recoil, proven already beneficial for $\bar{B} \rightarrow \bar{K}^*\ell^+\ell^-$ decays [12]. The low recoil framework is equally applicable to other B -meson to pseudo-scalar decays, including $\bar{B} \rightarrow \pi\ell^+\ell^-$, $\bar{B}_s \rightarrow \bar{K}\ell^+\ell^-$ and $\bar{B}_s \rightarrow \eta^{(\prime)}\ell^+\ell^-$. We find that the SM is presently in good agreement with the rare decay data.

Assuming none or negligible CP-violation only the current situation is shown in Fig. 7. The preferred confidence region is shared between disconnected islands, one including the SM. Only two, solution A and D, allow for a forward-backward asymmetry zero in $\bar{B}^0 \rightarrow \bar{K}^{*0}\ell^+\ell^-$ decays. We predict the location of the zero to be above 1.7 GeV^2 . If a zero is found, the

solution C, which is already disfavored, is excluded. Vice versa, if no zero is found, solutions A, the SM, and D are excluded. To distinguish the solutions A and D requires that the precision of the model-independent analysis reaches the level of being sensitive to interference terms with SM dominated four-fermion operators.

The presence of the pseudo-scalar channel improves the statistical power of the analysis. Even stronger advantages arise from correlations among the rare decays: We find that at low recoil the $\bar{B} \rightarrow \bar{K} \ell^+ \ell^-$ amplitude involves the same short-distance couplings present in $\bar{B} \rightarrow \bar{K}^* \ell^+ \ell^-$ for light leptons ($\ell = e$ or μ), and the corresponding CP-asymmetries in the rate, $a_{\text{CP}}^{(1)}$ as in Eq. (2.21), are identical. Moreover, the angular distribution in $\bar{B} \rightarrow \bar{K} \ell^+ \ell^-$ is an indicator for operators beyond Eq. (2.1). In this operator basis, $A_{\text{FB}}(\bar{B} \rightarrow \bar{K} \ell^+ \ell^-)$ vanishes and F_H^ℓ receives only small corrections of the order m_ℓ^2/m_B^2 , hence vanishes for practical purposes for the light leptons as well. These observables will therefore be important null tests for effects from BSM operators, complementing the search for $\bar{B}_s \rightarrow \mu^+ \mu^-$ decays and lepton non-universality by comparing $\bar{B} \rightarrow \bar{K} \ell^+ \ell^-$ observables into electrons with those into muons, e.g., [4].

Note added: During the completion of this work a systematic analysis of $\Delta B = 1$ constraints including low- and high- q^2 data on $\bar{B} \rightarrow \bar{K}^* \ell^+ \ell^-$ but without $\bar{B} \rightarrow \bar{K} \ell^+ \ell^-$ decays appeared [36]. The findings for the SM operator basis are qualitatively consistent with [12, 13] and the present work.

ACKNOWLEDGMENTS

We thank Frederik Beaujean for advice on multidimensional analyses, Hideki Miyake for uncovering a numerical instability in the calculation of $\bar{B} \rightarrow \bar{K} \ell^+ \ell^-$ observables in a prerelease version of EOS and Mikihiro Nakao for useful communications on Belle's $B \rightarrow K^{(*)} \ell^+ \ell^-$ measurements. We are thankful to the technical team of the Φ Do HPC cluster, without which we could not have performed our scans.

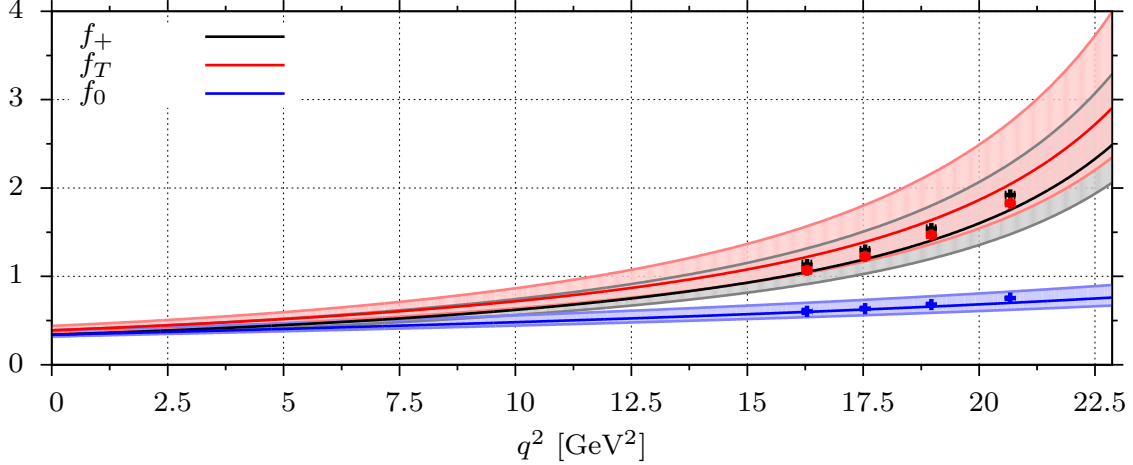


FIG. 9. The $\bar{B} \rightarrow \bar{K}$ form factors f_+ , f_T and f_0 by [7] extrapolated to the high- q^2 endpoint and preliminary lattice results with statistical uncertainties only (data points) [26]. The shaded bands show the respective form factor uncertainties.

Appendix A: The $B \rightarrow K$ form factors

The $B \rightarrow K$ form factors $f_{+,T,0}$ are defined as usual

$$\langle \bar{K}(k) | \bar{s} \gamma^\mu b | \bar{B}(p) \rangle = f_+(q^2) (p+k)^\mu + [f_0(q^2) - f_+(q^2)] \frac{m_B^2 - m_K^2}{q^2} q^\mu, \quad (\text{A1})$$

$$\langle \bar{K}(k) | \bar{s} \sigma^{\mu\nu} b | \bar{B}(p) \rangle = i \frac{f_T(q^2)}{m_B + m_K} [(p+k)^\mu q^\nu - q^\mu (p+k)^\nu], \quad (\text{A2})$$

where p (k) denotes the four-momentum of the B -meson (kaon) and $q = p - k$. The numerical analysis in this work is performed with the form factors from Ref. [7] parameterized as, $i = +, T, 0$

$$f_i(s) = \frac{f_i(0)}{1 - s/m_{\text{res},i}^2} \left\{ 1 + b_1^i \left(z(s) - z(0) + \frac{1}{2} (z(s)^2 - z(0)^2) \right) \right\}, \quad s = q^2, \quad (\text{A3})$$

$$z(s) = \frac{\sqrt{\tau_+ - s} - \sqrt{\tau_+ - \tau_0}}{\sqrt{\tau_+ - s} + \sqrt{\tau_+ - \tau_0}}, \quad \tau_0 = \sqrt{\tau_+} (\sqrt{\tau_+} - \sqrt{\tau_+ - \tau_-}), \quad \tau_\pm = (m_B \pm m_K)^2,$$

and the input given in Table IV. The values $f_i(q^2 = 0)$ stem from LCSR calculations. The form factors are shown in Fig. 9, extrapolated to high q^2 . Here, the agreement with preliminary lattice results by Liu *et al.* [26], which are shown as well, is good.

Form factors stemming from different methods and parameterizations relevant to $\bar{B} \rightarrow \bar{K} \ell^+ \ell^-$ decays at low recoil are compared in Fig. 10. Here we show f_+ and the ratio f_0/f_+ entering $\bar{B} \rightarrow \bar{K} \tau^+ \tau^-$ decays divided by the corresponding (extrapolated) ones used in our

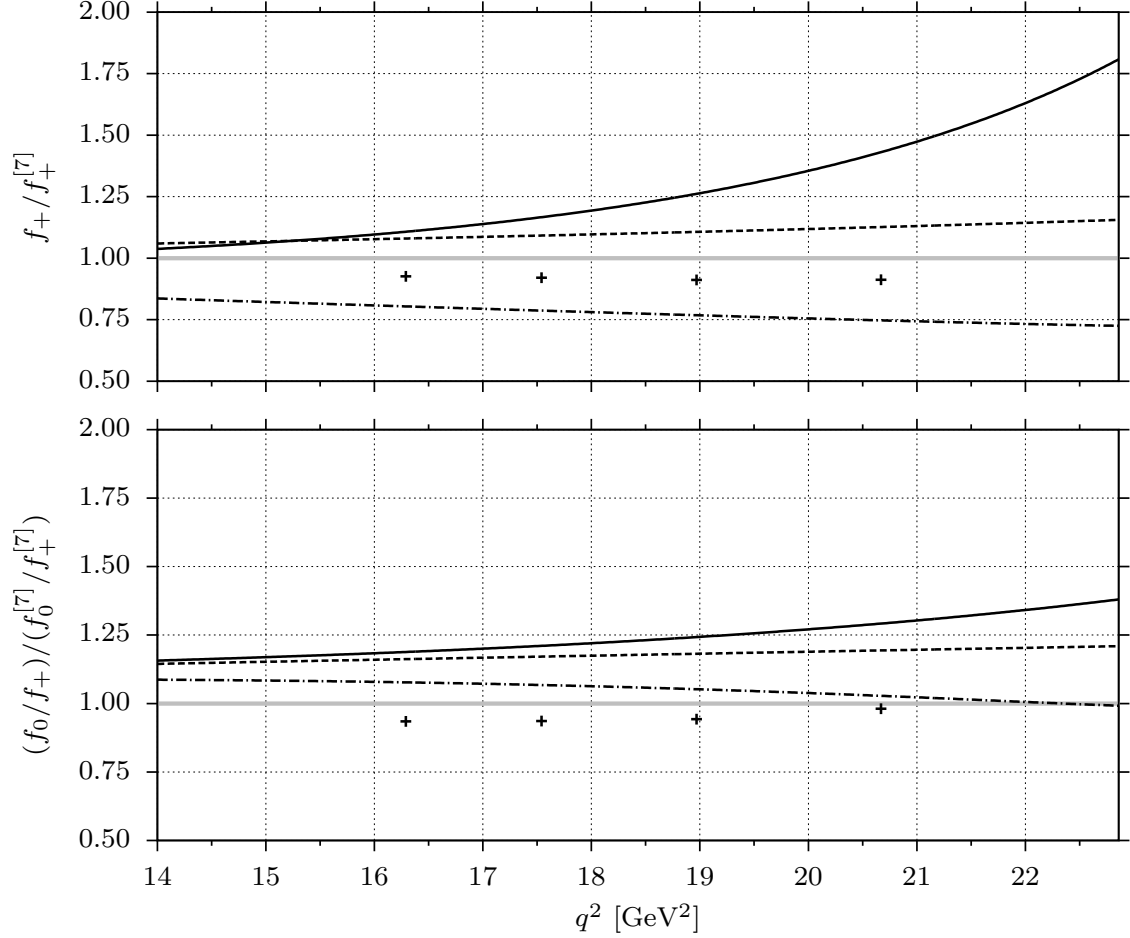


FIG. 10. Ratios of f_+ and f_0/f_+ from extrapolated LCSR by [37] (solid lines), extrapolated LCSR with simplified series expansion [38] (dashed), a relativistic quark model [39] (dash-dotted) and unquenched lattice calculations [26] (points), over the corresponding extrapolated form factors [7] used in this work.

analysis, from Ref. [7]. Owing to a different q^2 -shape the extrapolated LCSR ones from [37] (solid lines) grow much larger towards very low recoil, and differ most strongly from the findings of [7] and lattice [26]. Both findings for f_+ in the relativistic quark model [39] and LCSR from [37] combined with a simplified series expansion [38] exhibit a shape similar to the ones from [7]. The differences between f_+ and f_0/f_+ from [7] and [38, 39] are within 25% and 21%, respectively, which is within the uncertainties covered by Table IV.

The validity of the lowest order improved Isgur-Wise form factor relation Eq. (2.4) can be quantified by looking at deviations of

$$R_T(q^2) = \frac{q^2}{m_B(m_B + m_K)} \frac{f_T(q^2)}{f_+(q^2)} \quad (\text{A4})$$

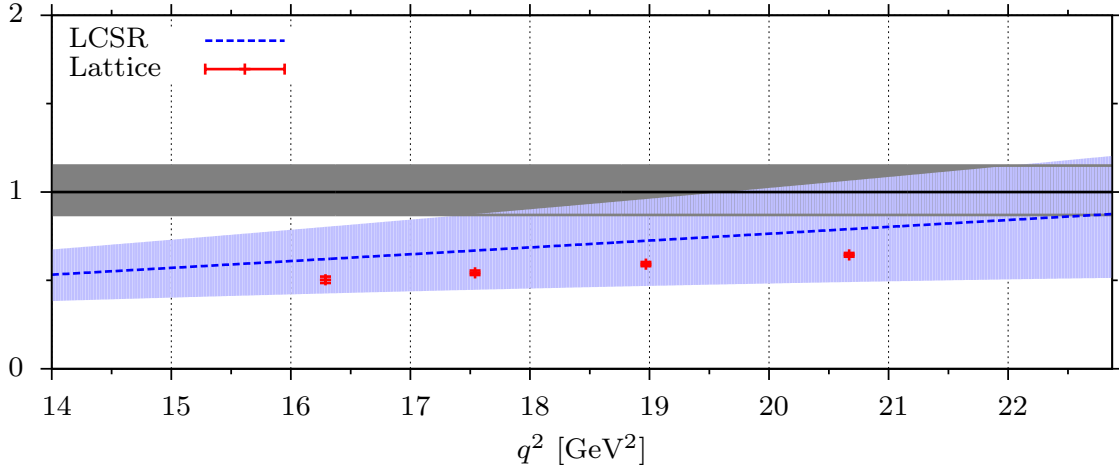


FIG. 11. The relation $R_T(q^2)$ given in Eq. (A4) from extrapolations of the LCSR form factors of [7] (blue band) and lattice [26] (red points). The grey band indicates the Λ/m_b -correction to Eq. (2.4), see text.

Form Factor f_i	Resonance	$f_i(0)$	b_1^i
f_+	$m_{\text{res},+} = 5.412 \text{ GeV}$	$0.34_{-0.02}^{+0.05}$	$-2.1_{-1.6}^{+0.9}$
f_0	no pole	$0.34_{-0.02}^{+0.05}$	$-4.3_{-0.9}^{+0.8}$
f_T	$m_{\text{res},T} = 5.412 \text{ GeV}$	$0.39_{-0.03}^{+0.05}$	$-2.2_{-2.0}^{+1.0}$

TABLE IV. Input to the $B \rightarrow K$ form factor parameterization Eq. (A3) from [7].

from κ , given in Eq. (2.5). As can be inferred from Fig. 11, for both the LCSR extrapolation [7] and lattice results [26] the agreement is good near the kinematical endpoint. For smaller dilepton masses R_T is smaller than $\kappa \simeq 1$. The agreement improves somewhat if the kinematical prefactor on the right-hand side of Eq. (A4) is replaced by one. Note that $R_T(q^2)$ obtained with the form factors from [37–39] behaves very similar to the one of [7]. Including a positive-valued $1/m_b$ HQET form factor $\delta_+^{(0)}(q^2)$, as, for instance, from [11], the ratio f_T/f_+ calculated from Eq. (2.3) would increase further. The form factors $\delta_{\pm}^{(0)}$ are defined in terms of the heavy b -quark field h_v as [11]

$$\langle \bar{K}(k) | \bar{s} i \overleftarrow{D}_\mu h_v | \bar{B}(p) \rangle = \delta_+^{(0)}(q^2)(p+k)_\mu + \delta_-^{(0)}(q^2)q_\mu. \quad (\text{A5})$$

Lattice studies for $B \rightarrow \pi$ [40] suggest that they are not larger than the estimate by dimensional analysis.

We recall that the impact of f_T on the $\bar{B} \rightarrow \bar{K} \ell^+ \ell^-$ decay observables at low recoil is

subleading. This hampers on one side the extraction of f_T from data, on the other side reduces the theoretical uncertainties. Ultimately it is desirable to know all form factors more precisely from lattice QCD, or other means.

-
- [1] C. Bobeth, G. Hiller and D. van Dyk, arXiv:1105.2659 [hep-ph], to appear in the Proceedings of DISCRETE2010 (La Sapienza, Rome), December 6th-11th 2010.
 - [2] A. Ali, P. Ball, L. T. Handoko and G. Hiller, Phys. Rev. D **61**, 074024 (2000) [arXiv:hep-ph/9910221].
 - [3] B. Aubert *et al.* [BABAR Collaboration], Phys. Rev. D **73**, 092001 (2006) [arXiv:hep-ex/0604007].
 - [4] C. Bobeth, G. Hiller and G. Piranishvili, JHEP **0712**, 040 (2007) [arXiv:0709.4174 [hep-ph]].
 - [5] M. Beneke, T. Feldmann and D. Seidel, Nucl. Phys. B **612** (2001) 25 [arXiv:hep-ph/0106067].
 - [6] M. Beneke, T. Feldmann and D. Seidel, Eur. Phys. J. C **41** (2005) 173 [arXiv:hep-ph/0412400].
 - [7] A. Khodjamirian, T. Mannel, A. A. Pivovarov and Y. M. Wang, JHEP **1009**, 089 (2010) [arXiv:1006.4945 [hep-ph]].
 - [8] B. Grinstein and D. Pirjol, Phys. Rev. D **70** (2004) 114005 [arXiv:hep-ph/0404250].
 - [9] M. Beylich, G. Buchalla and T. Feldmann, Eur. Phys. J. **C71** (2011) 1635 [arXiv:1101.5118 [hep-ph]].
 - [10] G. Buchalla and G. Isidori, Nucl. Phys. **B525**, 333-349 (1998) [hep-ph/9801456].
 - [11] B. Grinstein and D. Pirjol, Phys. Lett. B **533** (2002) 8 [arXiv:hep-ph/0201298].
 - [12] C. Bobeth, G. Hiller and D. van Dyk, JHEP **1007**, 098 (2010) [arXiv:1006.5013 [hep-ph]].
 - [13] C. Bobeth, G. Hiller and D. van Dyk, JHEP **1107**, 067 (2011) [arXiv:1105.0376 [hep-ph]].
 - [14] M. Patel, T. Blake for the [LHCb Collaboration], Conference report prepared for the 2011 Europhysics Conference on High-Energy Physics, LHCb-CONF-2011-038.
 - [15] T. Blake, [arXiv:1109.6582 [hep-ex]].
 - [16] A. Golutvin, Talk given at La Thuile 2011, LHCb-TALK-2011-029.
 - [17] T. Hurth and D. Wyler in J. L. Hewett *et al.*, arXiv:hep-ph/0503261.
 - [18] N. Isgur and M. B. Wise, Phys. Rev. **D42**, 2388-2391 (1990).
 - [19] D. A. Demir, K. A. Olive, M. B. Voloshin, Phys. Rev. **D66** (2002) 034015 [hep-ph/0204119].
 - [20] A. K. Alok, A. Dighe and S. Uma Sankar, Phys. Rev. **D78**, 114025 (2008) [arXiv:0810.3779]

- [hep-ph]].
- [21] P. Z. Skands, JHEP **0101**, 008 (2001) [arXiv:hep-ph/0010115].
- [22] EOS Collaboration, a code for flavor observables <http://project.het.physik.tu-dortmund.de/eos/>.
- [23] J. Charles *et al.* [CKMfitter Group Collaboration], Eur. Phys. J. **C41**, 1-131 (2005) [hep-ph/0406184]. We use the numerical results as presented at ICHEP10.
- [24] K. Nakamura *et al.* [Particle Data Group], J. Phys. G **37**, 075021 (2010).
- [25] [Tevatron Electroweak Working Group and CDF Collaboration and D0 Collab], arXiv:0903.2503 [hep-ex].
- [26] Z. Liu, S. Meinel, A. Hart, R. R. Horgan, E. H. Muller and M. Wingate, [arXiv:1101.2726 [hep-ph]].
- [27] J. T. Wei *et al.* [BELLE Collaboration], Phys. Rev. Lett. **103**, 171801 (2009) [arXiv:0904.0770 [hep-ex]].
- [28] T. Aaltonen *et al.* [CDF Collaboration] [arXiv:1107.3753 [hep-ex]].
- [29] U. Egede, T. Hurth, J. Matias, M. Ramon and W. Reece, JHEP **0811**, 032 (2008) [arXiv:0807.2589 [hep-ph]].
- [30] J. Walsh, Talk given at the 46th Rencontres de Moriond: Electroweak Interactions and Unified Theories 2011, (La Thuile), March 13th-20th 2011.
- [31] T. Aaltonen *et al.* [CDF Collaboration], arXiv:1108.0695 [hep-ex].
- [32] C. Wacker, Diploma Thesis, TU Dortmund, November 2011.
- [33] G. Hiller, arXiv:1106.1547 [hep-ph], to appear in the proceedings of the 46th Rencontres de Moriond: Electroweak Interactions and Unified Theories 2011, (La Thuile), March 13th-20th 2011.
- [34] A. Ali, G. Kramer and G. -h. Zhu, Eur. Phys. J. **C47**, 625-641 (2006) [hep-ph/0601034].
- [35] P. Ball and R. Zwicky, Phys. Rev. **D71**, 014029 (2005) [hep-ph/0412079].
- [36] W. Altmannshofer, P. Paradisi and D. Straub, arXiv:1111.1257 [hep-ph].
- [37] P. Ball and R. Zwicky, Phys. Rev. **D71**, 014015 (2005) [hep-ph/0406232].
- [38] A. Bharucha, T. Feldmann and M. Wick, JHEP **1009**, 090 (2010) [arXiv:1004.3249 [hep-ph]].
- [39] A. Faessler, T. Gutsche, M. A. Ivanov, J. G. Korner and V. E. Lyubovitskij, Eur. Phys. J. direct **C4**, 18 (2002) [hep-ph/0205287].
- [40] E. Dalgic *et al.*, Phys. Rev. **D73**, 074502 (2006) [hep-lat/0601021].